Electronic Supplementary Material (ESI) for Dalton Transactions.
This journal is © The Royal Society of Chemistry 2020

Supporting Information

Retention of Anions in Cobalt Hydroxide with Ni Substitution to Emphasize Role of Anion and Cations for High Current Density in Oxygen Evolution Reaction

Umair Shamraiz [1*], Rukhsana Gul[2], Amin Badshah[1], Bareera Raza[3]

[1]Department of Chemistry and Department of Environmental Sciences, Quid-i-Azam University, Islamabad 4300, Pakistan

[2]Department of Chemistry, Kohat University of science and Technology, KOHAT

[3]Shanghai Electrochemical Energy Devices Research Center, School of Chemistry and Chemical Engineering, Shanghai Jiatong University, Shanghai, 200240, China

Corresponding Author: umairshamraiz@gmail.com

Turnover frequency for an electrocatalytic water splitting reactions can be evaluated by different means, in our case we have chosen the method of using OER current at specific over voltage and the surface concentration of catalyst atoms at the modified Nickel foam working electrode which was calculated from the amount of the catalyst we added to modify the working electrode. The corresponding expression as:

TOF = *i*×NA / A × F × n × Γ

Where, i = current NA= Avogadro number A = Geometrical surface area of the electrode F = Faraday constant n = Number of electrons Γ = Surface concentration. We have taken the OER current observed at 1.50 V (vs. RHE) and calculated the TOF to be 0.07 s^{-1}, 0.78 s^{-1}, 11.7 s^{-} for β-$Co(OH)_2$/NF, α-$Co(OH)_2$/NF, and α-CoNiOOH/NF, respectively shown in Figure S7.

Furthermore, electrical double layer capacitance (EDLC) was used to evaluate the capacitive behavior of the synthesized electrocatalysts for practical applications. Furthermore, Figure S8 a, c & e illustrates the cyclic voltammograms for α-CoNiOOH/NF, α-$Co(OH)_2$/NF, and β-$Co(OH)_2$/NF, respectively at various scan rates from (100-500 mVs^{-1}) in the non-faradaic region between 0.9-1.0 V (vs RHE). A rectangular behavior was observed for all the synthesized catalysts, which confirms the existence of a double layer. Furthermore, a linear increase in both the anodic (i_a) and cathodic (i_c) current densities was observed with increase in scan rate. The capacitance of α-CoNiOOH/NF is 7.76 $mFcm^{-2}$ which is higher than the capacitance for α-$Co(OH)_2$/NF i.e. 5.72 $mFcm^{-2}$, which is analogous with the other results.

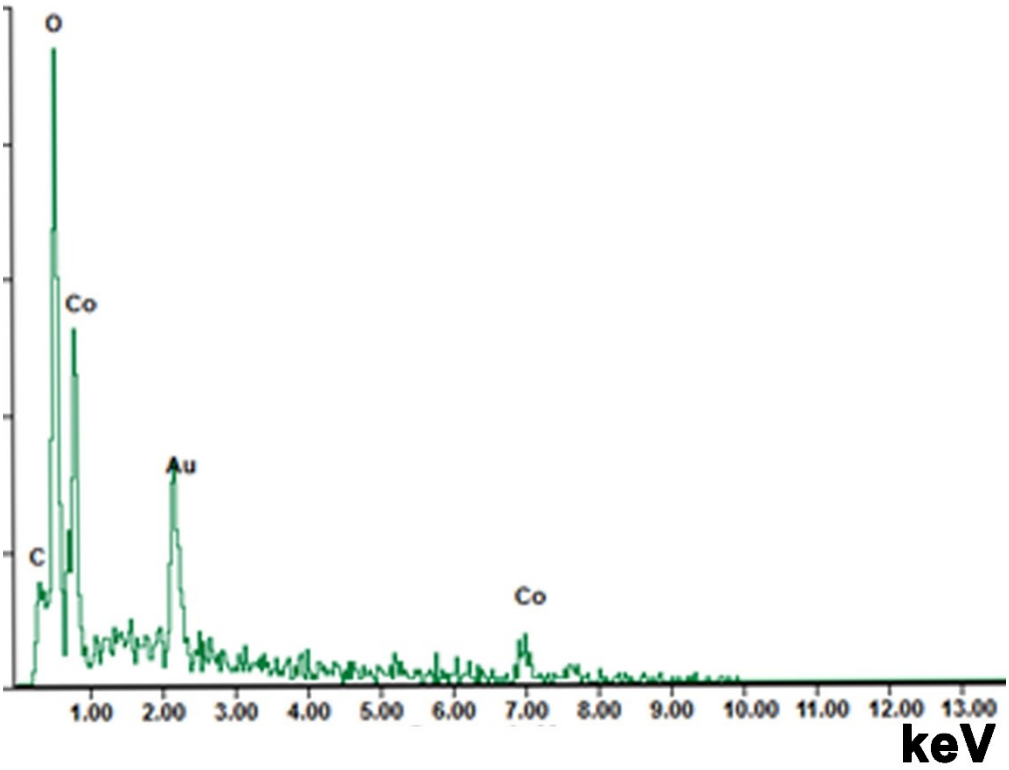

Figure S1. Representative EDX spectrum of β-$Co(OH)_2$.

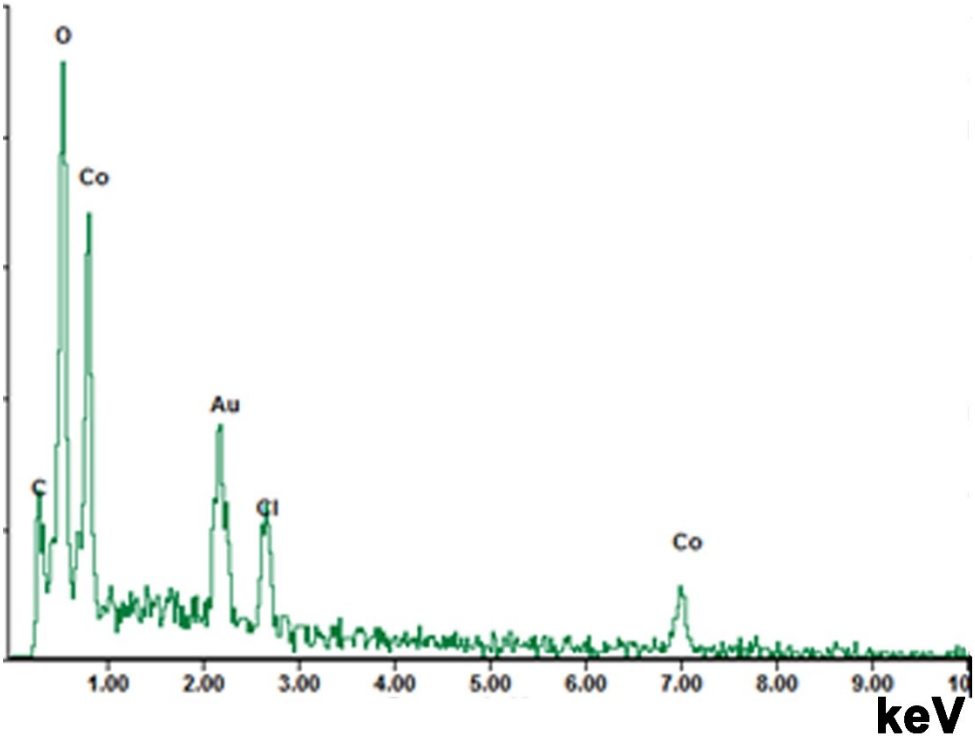

Figure S2. Representative EDX spectrum of α- $Co(OH)_2$.

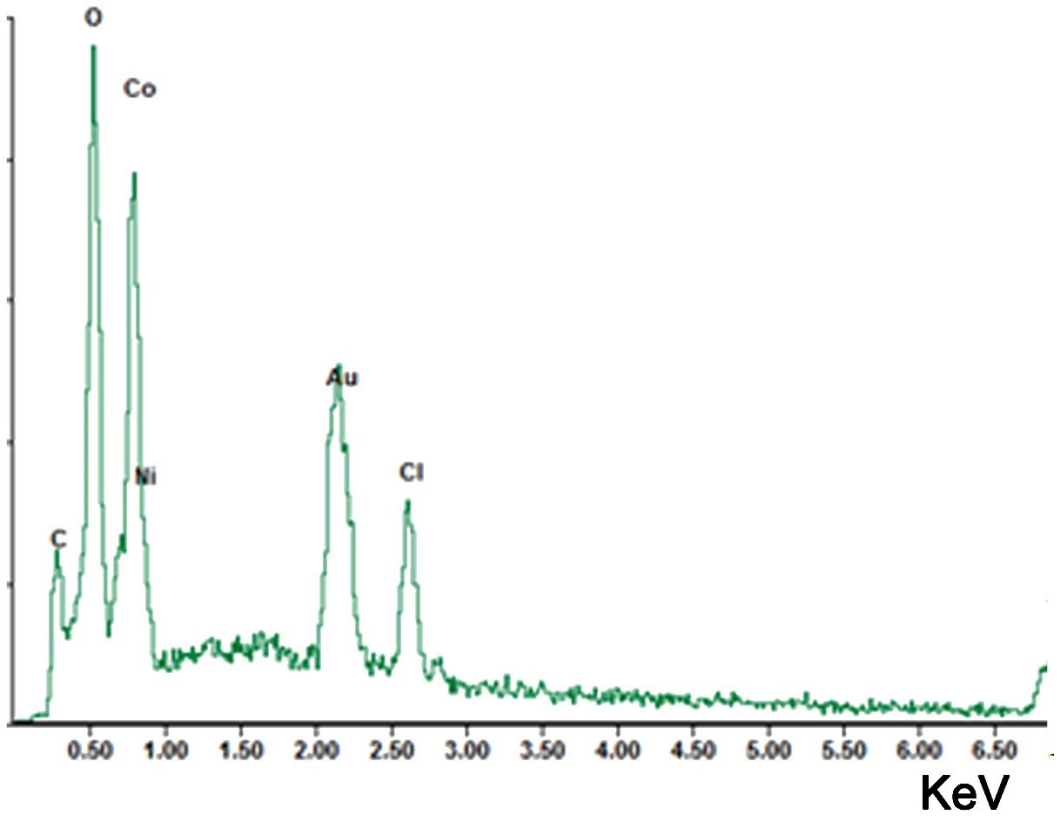

Figure S3. Representative EDX spectrum of α-CoNiOOH.

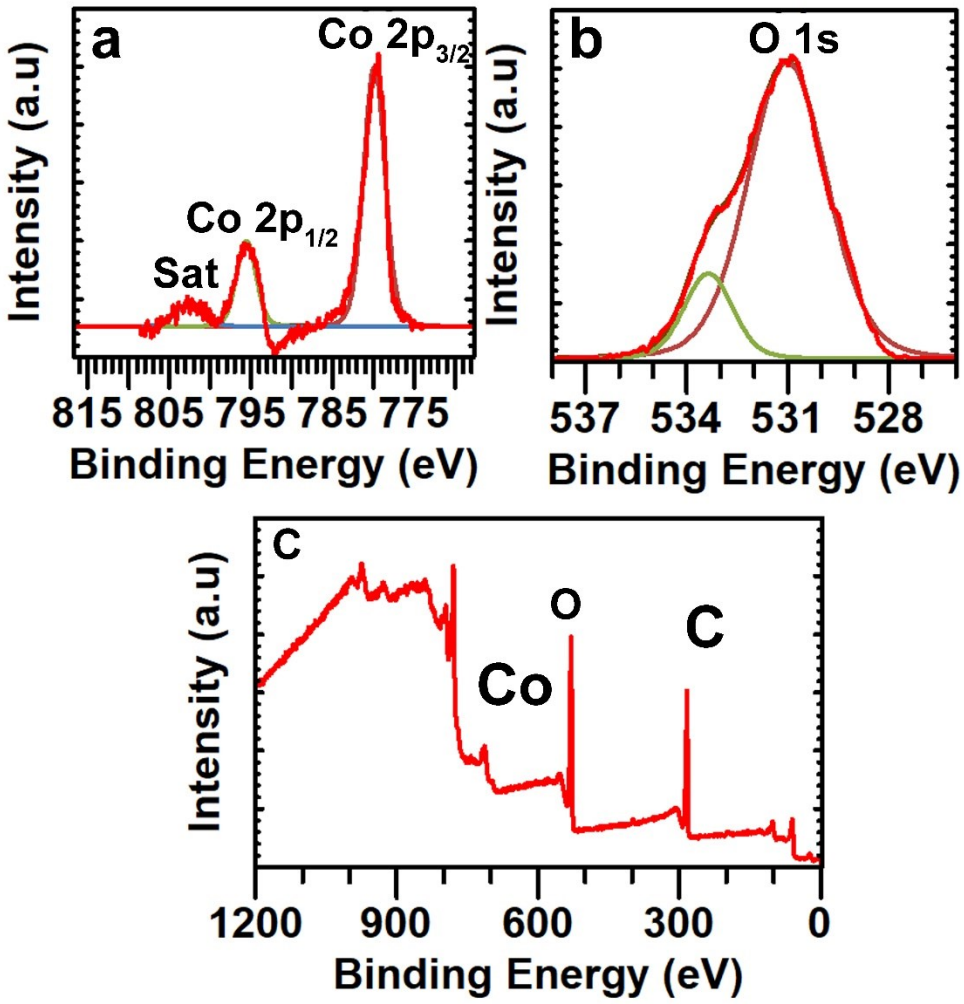

Figure S4. XPS analysis of β- $Co(OH)_2$. **(a)** Co. **(b)** O. **(c)** Complete XPS.

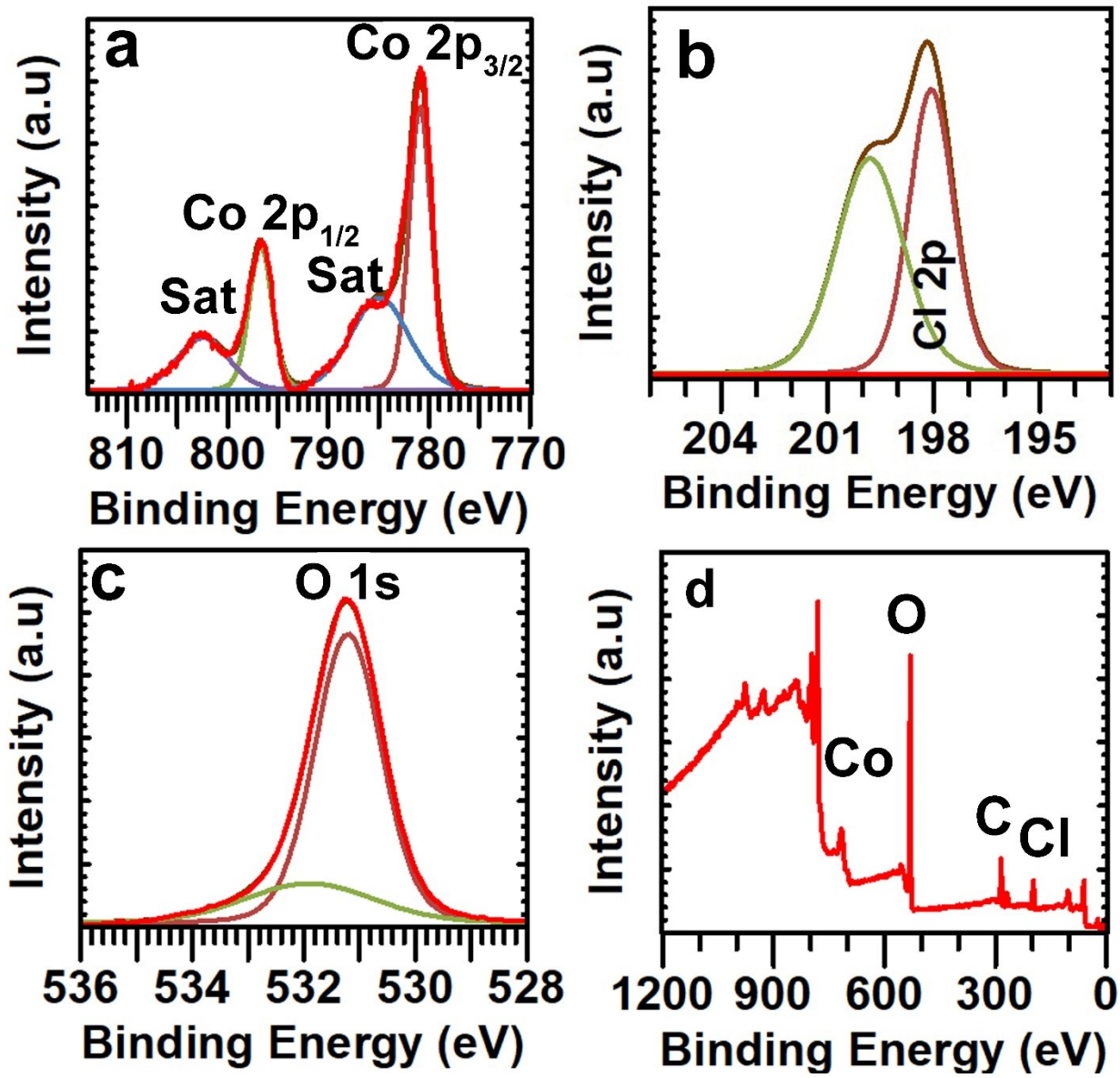

Figure S5. XPS analysis of α-$Co(OH)_2$. **(a)** Co. **(b)** Cl. **(c)** O. **(d)** Complete XPS.

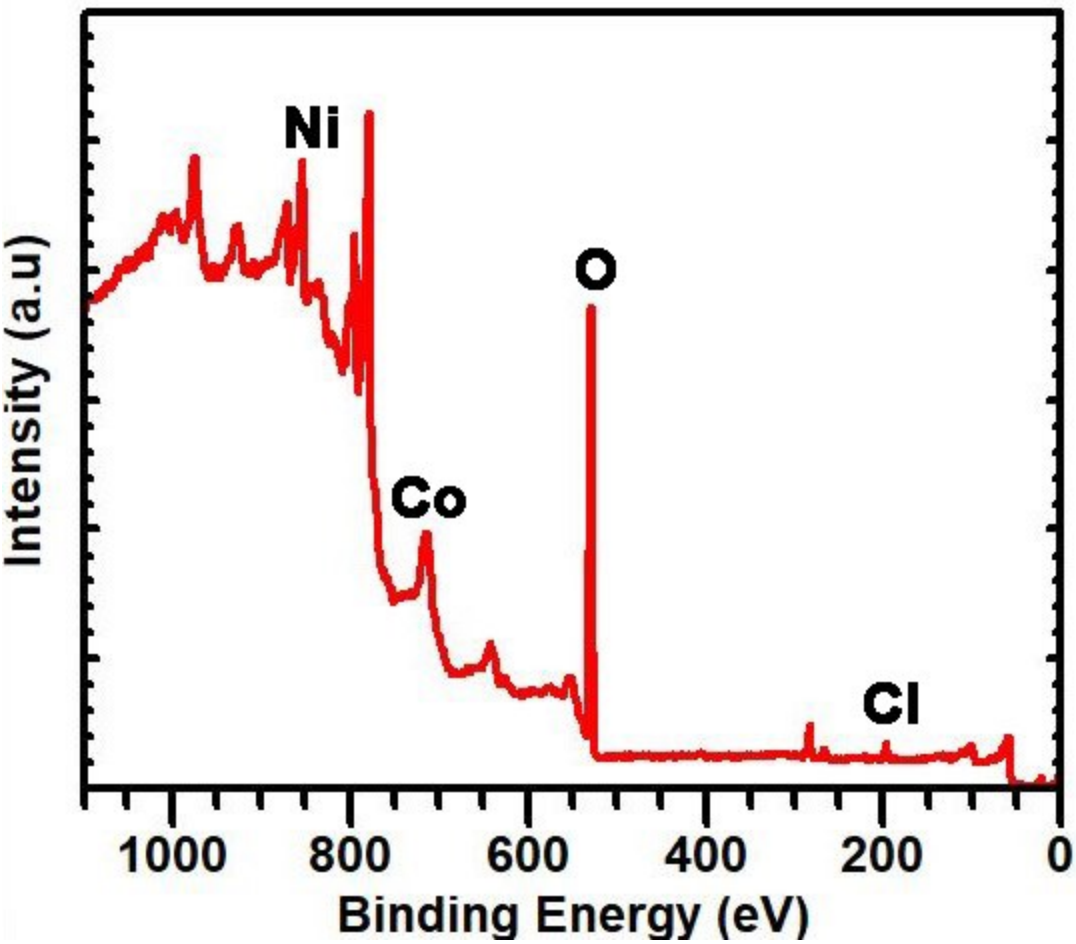

Figure S6. Complete XPS spectrum of α-CoNiOOH

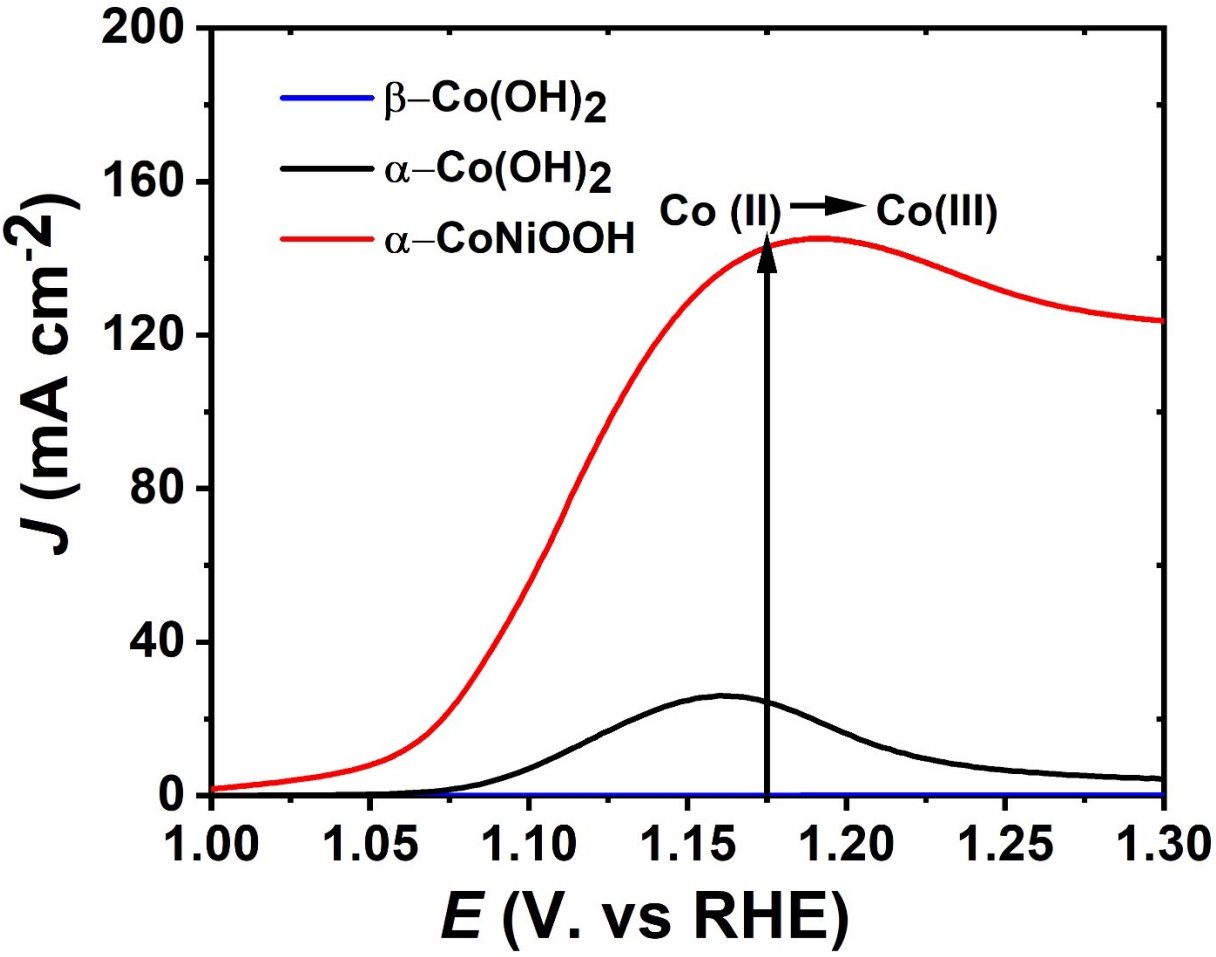

Figure S7. Conversion of Co(II)-Co(III) during electrocatalysis.

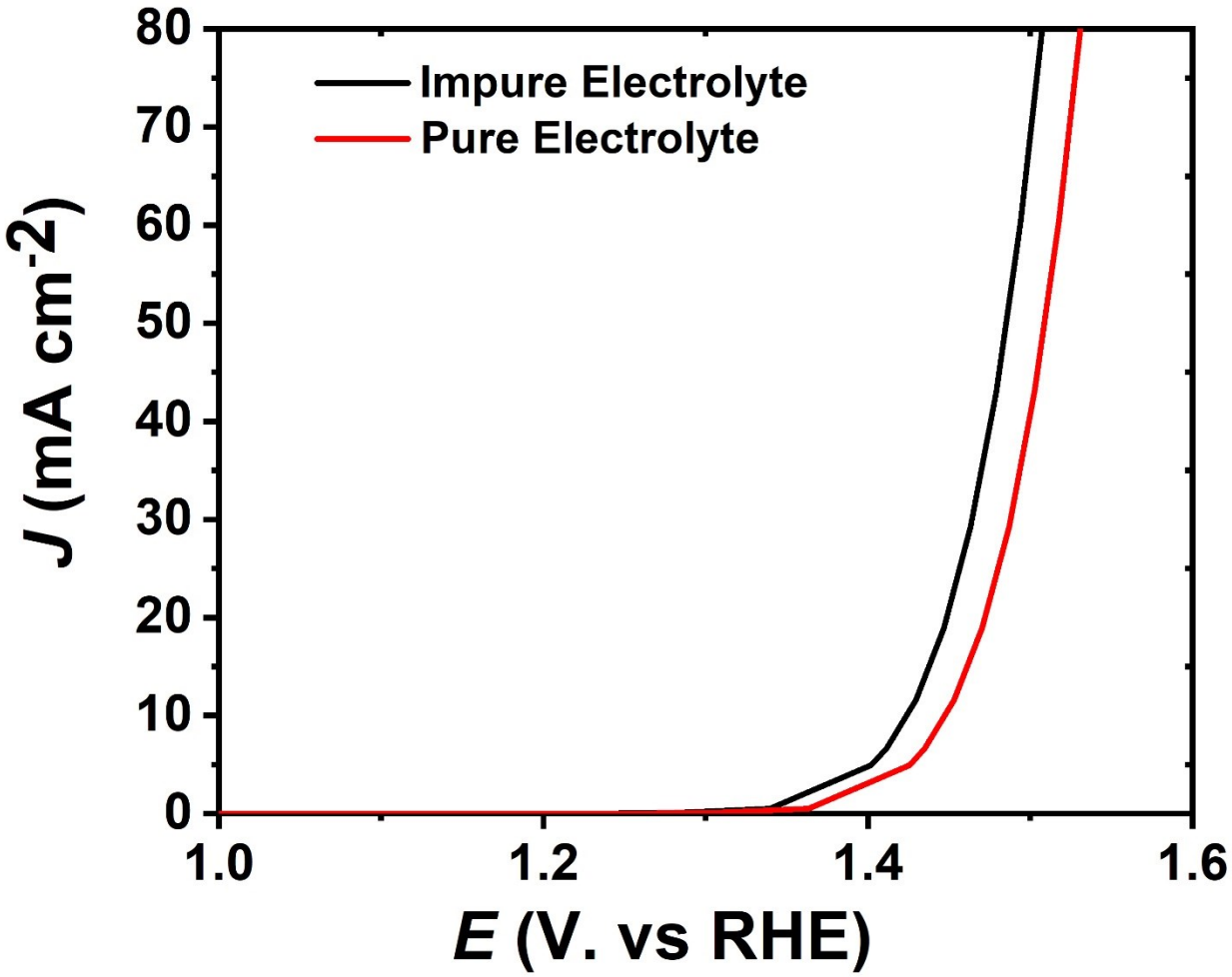

Figure S8. Linear sweep voltammograms of α-CoNiOOH in pure and impure electrolyte for OER activity.

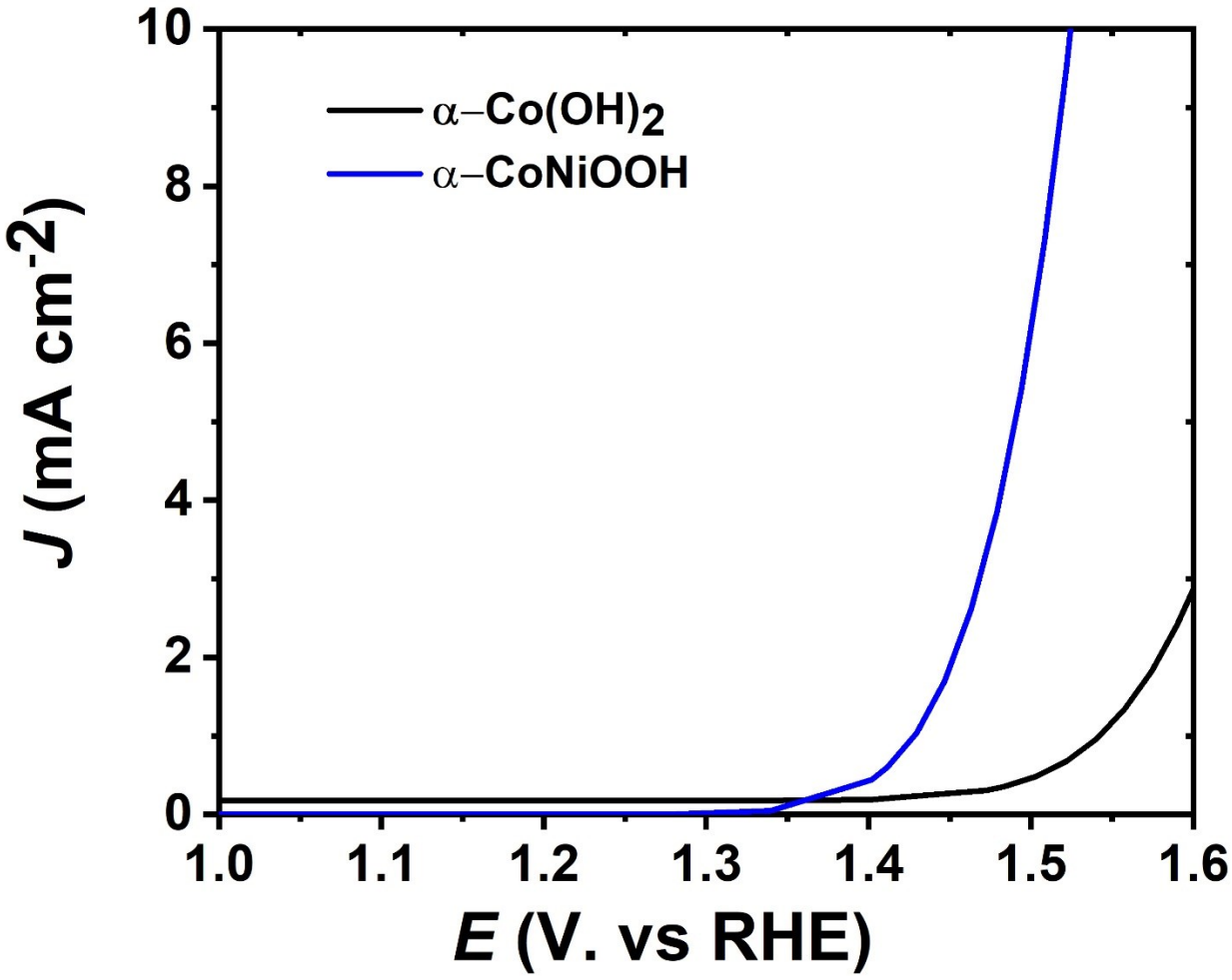

Figure S9. Linear Sweep Voltammograms normalized to ECSA.

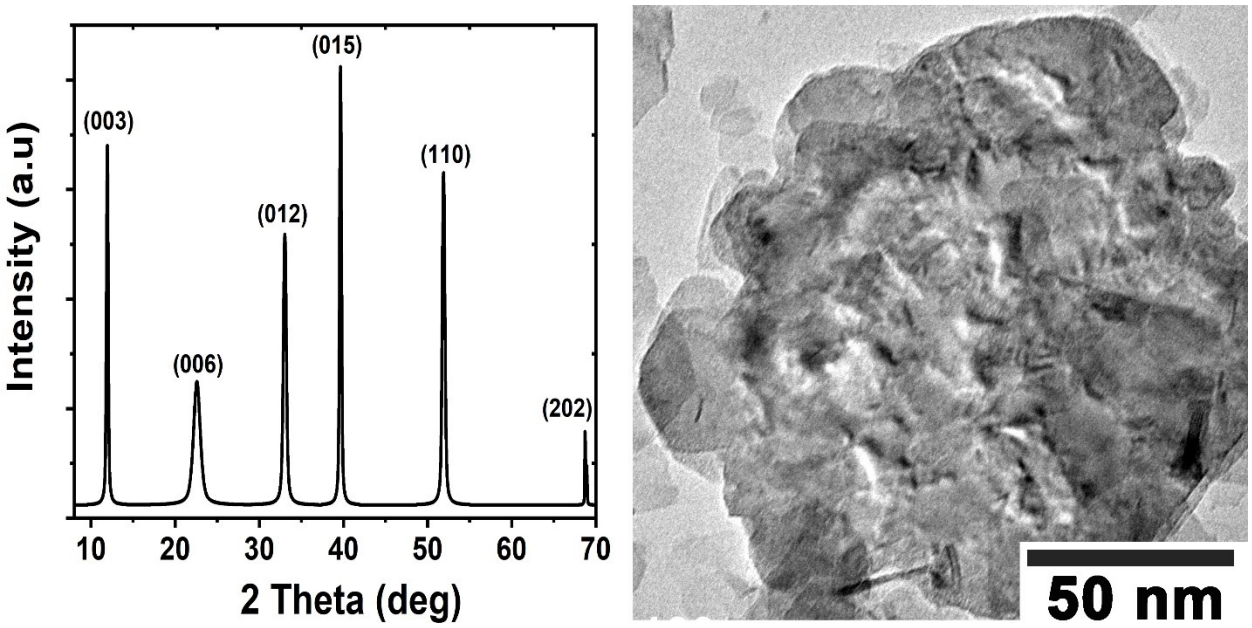

Figure S10. The PXRD and TEM after stability for 24 h.

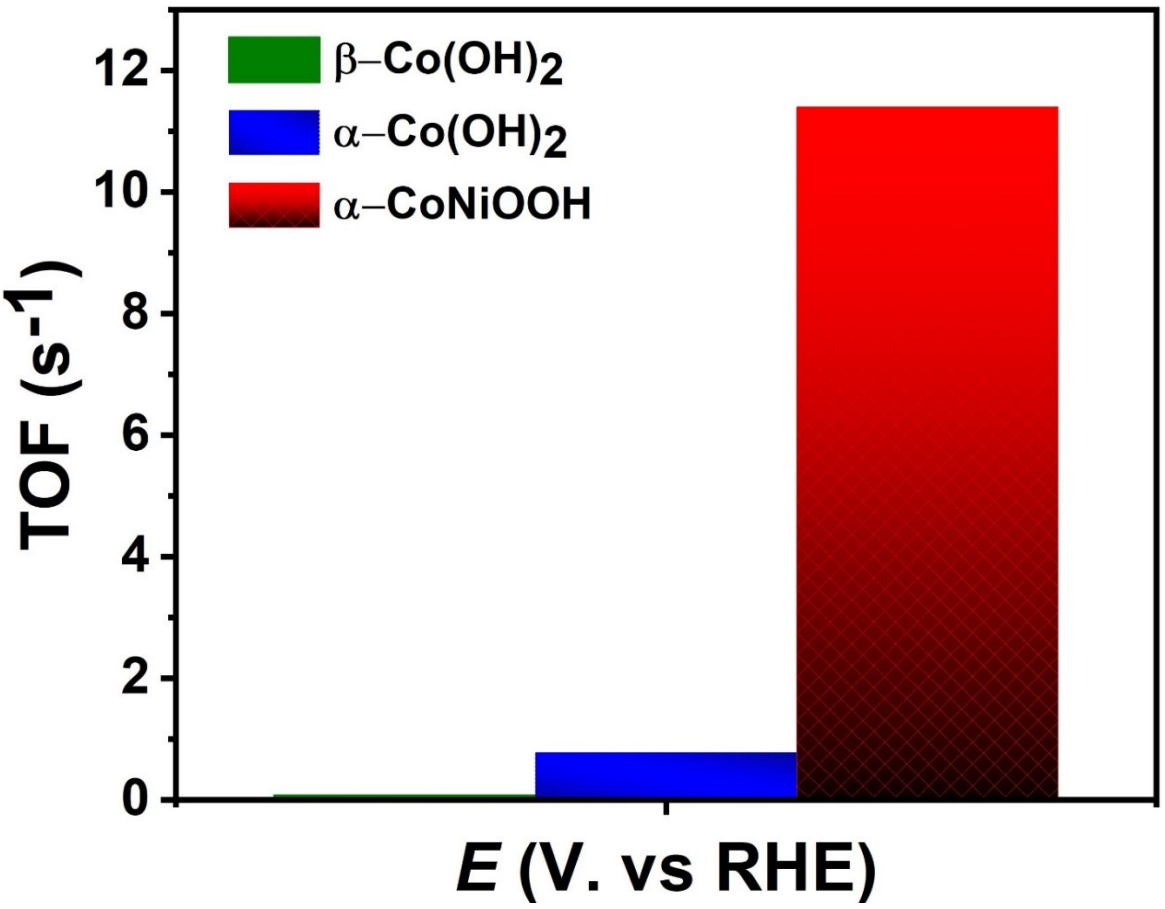

Figure S11. Turnover Frequency of the Electrocatalysts.

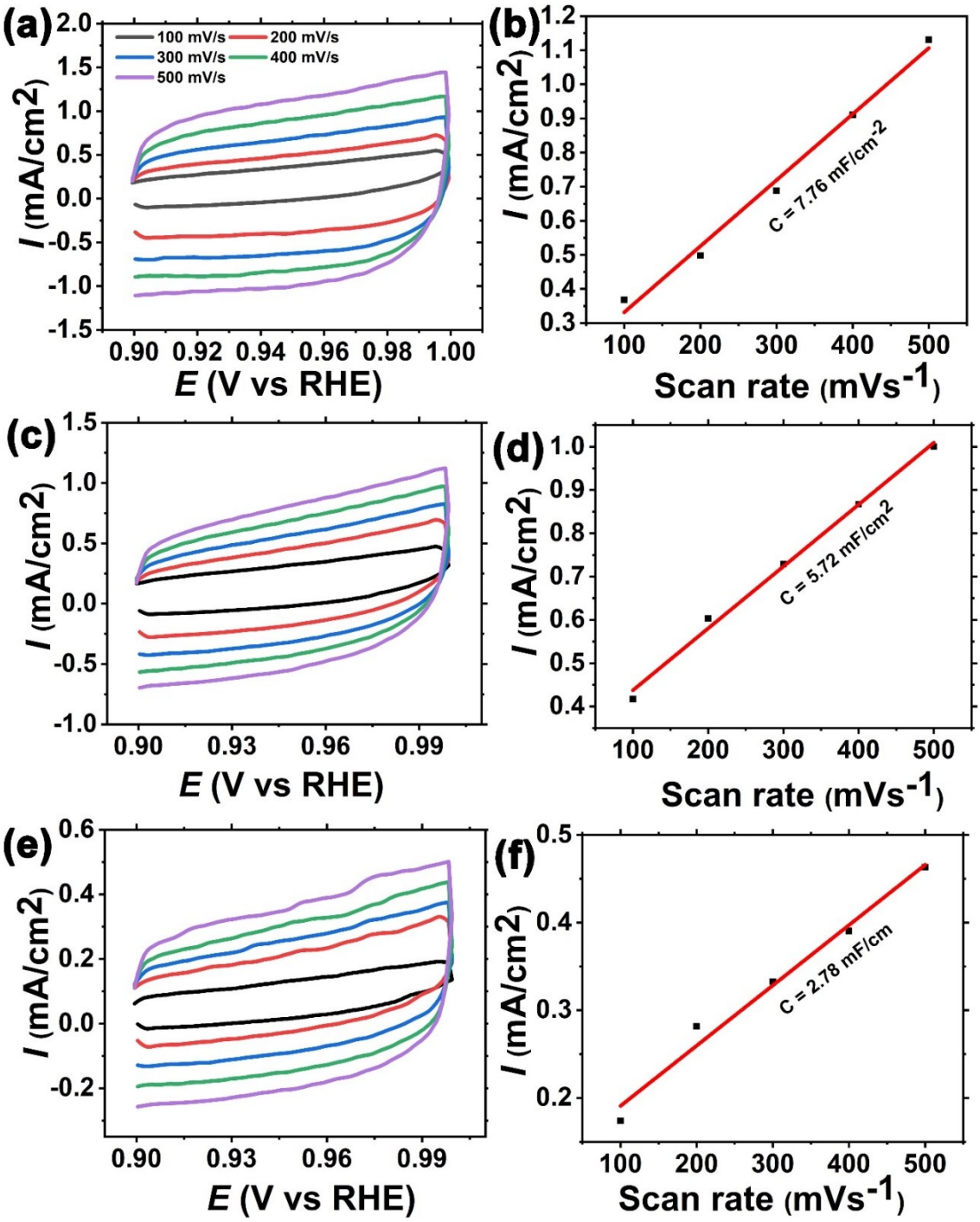
(a)
100 mV/s
200 mV/s
300 mV/s
400 mV/s
500 mV/s
I (mA/cm2)
E (V vs RHE)
(b)
I (mA/cm2)
C = 7.76 mF/cm-2
Scan rate (mVs-1)
(c)
I (mA/cm2)
E (V vs RHE)
(d)
I (mA/cm2)
C = 5.72 mF/cm2
Scan rate (mVs-1)
(e)
I (mA/cm2)
E (V vs RHE)
(f)
I (mA/cm2)
C = 2.78 mF/cm
Scan rate (mVs-1)

Figure S12. Cyclic voltammograms of electrodes at the scan rate of 100, 200, 300, 400 and 500 mV s^{-1} in 1 M KOH. **(a)** α-Co_2NiOOH/NF. **(c)** β-CoOOH/NF. **(e)** α-CoOOH/NF. **(b, d & f)** Linear fitted curve of corresponding capacitive currents at 0.94 V (vs. RHE).

Table S1. BET surface area and pore volume of α-$Co(OH)_2$, β-$Co(OH)_2$, and α-CoNiOOH

Material	BET Surface Area m^2/g	Langmuir Surface Area m^2/g	BJH Pore Volume (cm^3/g)	BET Pore Size (Å)
β-$Co(OH)_2$	40.62	272.90	0.16	88.33
α-$Co(OH)_2$	87.78	292.01	0.28	56.78
α-CoNiOOH	134.29	772.39	0.30	43.40

Table S2. A comparison of OER catalysts at 10 mA cm^{-2}

Catalyst	η^{10} (mV)	Electrolyte	Ref
α-Co_2NiOOH	190	1M KOH	**This Work**
CoZn LDH	470	0.1M KOH	[1]
CoMn LDH	293	1M KOH	[2]
CoFe LDH	314	1M KOH	[3]
$Fe_{0.1}NiS_2$ NA/Ti	205	1M KOH	[4]
$Ni_{2.3\%}CoS_2$/CC	297	1M KOH	[5]
Ag NP/NiRu-LDHs	310	0.1M KOH	[6]

OCoCCuxNiyFe4-x-yN/NF	121	0.1M KOH	[7]
CoFe/NF	220	1M KOH	[8]
Co-Ni_3N	307	1M KOH	[9]
CcNiFeMo	238	1M KOH	[10]
$Ni_{0.75}Fe_{0.125}V_{0.125}$-LDHs/ NF	231	1M KOH	[11]
CoFePO	274.5	1M KOH	[12]

References

[1] C. Qiao, Y. Zhang, Y. Zhu, C. Cao, X. Bao, J. Xu, *J. Mater. Chem. A* **2015**, *3*, 6878.

[2] F. Song, X. Hu, *J. Am. Chem. Soc.* **2014**, *136*, 16481.

[3] A. M. P. Sakita, R. Della, E. Vallés, A. V Benedetti, *Appl. Surf. Sci.* **2018**, *434*, 1153.

[4] N. Yang, C. Tang, K. Wang, G. Du, A. M. Asiri, X. Sun, *Nano Res.* **2016**, *9*, 3346.

[5] T. Liu, A. M. Asiri, X. Sun, *Nanoscale* **2016**, *8*, 3911.

[6] S. A. Chala, M. C. Tsai, W. N. Su, K. B. Ibrahim, A. D. Duma, M. H. Yeh, C. Y. Wen, C. H. Yu, T. S. Chan, H. Dai, B. J. Hwang, *ACS Catal.* **2019**, *9*, 117.

[7] L. Gan, L. Hu, H. An, J. Fang, Y. Lai, J. Li, *ACS Appl. Mater. Interfaces* **2018**, *10*, 41465.

[8] P. Babar, A. Lokhande, H. H. Shin, B. Pawar, M. G. Gang, S. Pawar, J. H. Kim, *Small* **2018**, *14*, 1.

[9] C. Zhu, A. L. Wang, W. Xiao, D. Chao, X. Zhang, N. H. Tiep, S. Chen, J. Kang, X. Wang, J. Ding, J. Wang, H. Zhang, H. J. Fan, *Adv. Mater.* **2018**, *30*, 1.

[10] F. Qin, Z. Zhao, M. K. Alam, Y. Ni, F. Robles-Hernandez, L. Yu, S. Chen, Z. Ren, Z. Wang, J. Bao, *ACS Energy Lett.* **2018**, *3*, 546.

[11] K. N. Dinh, P. Zheng, Z. Dai, Y. Zhang, R. Dangol, Y. Zheng, B. Li, Y. Zong, Q. Yan, *Small* **2018**, *14*, 1.

[12] J. Duan, S. Chen, A. Vasileff, S. Z. Qiao, *ACS Nano* **2016**, *10*, 8738.